PROCEEDINGS A

rspa.royalsocietypublishing.org

Research

Article submitted to journal

Subject Areas:
35J05,74J05,82D25

Keywords:
Acoustic Radiation Potential, Crystallographic symmetries, Bravais lattices, Ultrasound Directed Self-Assembly

Author for correspondence:
Fernando Guevara Vasquez
e-mail: fguevara@math.utah.edu

THE ROYAL SOCIETY
PUBLISHING

Periodic particle arrangements using standing acoustic waves

Fernando Guevara Vasquez[1] and China Mauck[1]

[1]Mathematics Department, University of Utah, Salt Lake City UT 84112, USA

We determine crystal-like materials that can be fabricated by using a standing acoustic wave to arrange small particles in a non-viscous liquid resin, which is cured afterwards to keep the particles in the desired locations. For identical spherical particles with the same physical properties and small compared to the wavelength, the locations where the particles are trapped correspond to the minima of an acoustic radiation potential which describes the net forces that a particle is subject to. We show that the global minima of spatially periodic acoustic radiation potentials can be predicted by the eigenspace of a small real symmetric matrix corresponding to its smallest eigenvalue. We relate symmetries of this eigenspace to particle arrangements composed of points, lines or planes. Since waves are used to generate the particle arrangements, the arrangement's periodicity is limited to certain Bravais lattice classes that we enumerate in two and three dimensions.

1. Introduction

We are interested in characterizing the possible periodic or crystal-like materials that can be fabricated by using ultrasound directed self-assembly [1,2]. In this fabrication method, a liquid resin containing small particles is placed in a reservoir that is lined by ultrasound transducers. By operating the transducers at a fixed frequency, a standing acoustic wave is generated in the liquid and drives the particles to certain locations. For example, when the particles are neutrally buoyant and less compressible than the surrounding fluid, the particles tend to go to the wave nodes (zero amplitude locations), as we explain later. Once the particles are in the desired positions, the resin is cured (i.e. hardened with light, a curing agent, etc.) and we obtain a material with inclusions placed in a periodic fashion.

To give a rough idea, one could use this technique to fabricate a crystal-like material (essentially a grating) that selectively reflects millimetre waves, i.e. electromagnetic waves with wavelengths of the order of 1mm to 1cm. Indeed, one could achieve this by placing sub-wavelength metallic particles periodically inside a dielectric resin matrix. If we assume the speed of sound in the resin matrix is 1500ms^{-1}, we can expect the particles to be separated by between 5μm and 50μm provided the transducer operating frequency is between 150kHz and 1.5MHz. This rough estimate is based on a spacing of half an ultrasound wavelength that we rigorously justify later. A simple motivation, for now, is to observe that in one dimension there are actually two nodes of the wave per wavelength. We emphasize though that our analysis is valid in the case where the particles do not cluster about the wave nodes and holds in two or three dimensions.

The use of acoustic waves for manipulating particles has been widely studied, especially for applications to microfluidics [3,4] and for use as acoustic tweezers [5–7], which have particular appeal as a biomedical tool [8]. Other applications include single-cell patterning using surface acoustic waves [9], tissue engineering [10], and fabrication of laminates [11]. Additionally, acoustically configurable crystals were already considered in [12,13]. Our work shows the theoretical limits of manipulation of particles with standing acoustic waves in the particular case where the desired particle patterns are periodic. We derive explicit control strategies to obtain different crystallographic symmetries and give easy to check criteria to predict whether the acoustic traps occur on isolated points, lines or planes.

For our study we assume that acoustic waves at a fixed frequency f propagate in a fluid. The pressure and fluid velocity fields have the form $\widetilde{p}(\boldsymbol{x},t)=\Re(\exp[-i\omega t]p(\boldsymbol{x}))$ and $\widetilde{\boldsymbol{v}}(\boldsymbol{x},t)=\Re(\exp[-i\omega t]\boldsymbol{v}(\boldsymbol{x}))$ at position $\boldsymbol{x}\in\mathbb{R}^d$ ($d=2$ or 3) and time t. Here $\omega=2\pi f$ is the angular frequency and $\Re$ denotes the real part of a complex quantity. The time domain pressure and fluid velocity are related by

$$\begin{aligned}\widetilde{p}_t+\kappa_0\nabla\cdot\widetilde{\boldsymbol{v}}=0,\ \text{and}\\ \rho_0\widetilde{\boldsymbol{v}}_t+\nabla\widetilde{p}=0,\end{aligned}\tag{1.1}$$

where κ_0 is the compressibility of the fluid and ρ_0 its mass density. By using the expressions for $\widetilde{p}$ and $\widetilde{\boldsymbol{v}}$ in (1.1), we see that the frequency domain pressure p is a complex valued solution to the Helmholtz equation $\Delta p+k^2p=0$, where the wavenumber is $k=\omega/c$, and $c=\sqrt{\kappa_0/c_0}$ is the velocity of propagation of acoustic waves in the fluid (see e.g. [14]). Notice that the pressure and velocities in the frequency domain are related by $\boldsymbol{v}=(i\omega\rho_0)^{-1}\nabla p$.

(a) The acoustic radiation potential

Small (compared to the wavelength) particles in a fluid are subject to an acoustic radiation force [15–18]. It is convenient to study the average of this force over a time period $T=1/f$. To be more precise, the time average over a period of $T-$periodic function g is

$$\langle g\rangle=\frac{1}{T}\int_0^T g(t)dt.$$

The net acoustic radiation force experienced by a small particle and averaged over a time period is proportional to $\boldsymbol{F}=-\nabla\psi$, where $\psi(\boldsymbol{x})$ is the so-called acoustic radiation potential. For small spherical particles of fixed size, the acoustic radiation potential is given by[1]

$$\psi=\mathfrak{f}_1\frac{\kappa_0}{2}\left\langle|\widetilde{p}|^2\right\rangle-\mathfrak{f}_2\frac{3\rho_0}{4}\left\langle|\widetilde{\boldsymbol{v}}|^2\right\rangle,\tag{1.2}$$

where $\mathfrak{f}_1=1-(\kappa_p/\kappa_0)$ and $\mathfrak{f}_2=2(\rho_p-\rho_0)/(2\rho_p+\rho_0)$ are non-dimensional constants depending on the compressibilities of the particle and the fluid (κ_p and κ_0, respectively) and on their mass densities (ρ_p and ρ_0, respectively).

Since the net forces point in the direction of the negative gradient of the potential ψ, the particles tend to *cluster at the minima of the potential* ψ. The acoustic radiation potential can be

[1]We denote by $|\boldsymbol{v}|=(|v_1|^2+\ldots+|v_d|^2)^{1/2}$ the Euclidean norm of a vector $\boldsymbol{v}$ with d entries.

rewritten in terms of the frequency domain pressure as follows[2]

$$\psi = \mathfrak{a}|p|^2 - \mathfrak{b}|\nabla p|^2 = \begin{bmatrix} p \\ \nabla p \end{bmatrix}^* \begin{bmatrix} \mathfrak{a} & \\ & -\mathfrak{b}\mathsf{I}_d \end{bmatrix} \begin{bmatrix} p \\ \nabla p \end{bmatrix}, \tag{1.3}$$

where $\mathfrak{a} = \mathfrak{f}_1\kappa_0/4$, $\mathfrak{b} = \mathfrak{f}_2 3/(8\rho_0\omega^2)$, I_d is the $d \times d$ identity matrix and $*$ denotes the conjugate transpose. The key observation here is that for fixed $\boldsymbol{x}$, we can think of the acoustic radiation potential as a quadratic form in p and ∇p. We make no particular assumption on the signs of $\mathfrak{a}$ and $\mathfrak{b}$, as they depend on the physical properties of the particles and the fluid.

Remark 1.1. In general the acoustic radiation potential depends also on the size and shape of the particles, thus by using (1.2) to predict where the particles cluster, we are neglecting the effect of the particle's size and shape.

Remark 1.2. Optical forces analogous to the acoustic radiation force can be used to trap particles in crystal-like formations called optical lattices, which can be obtained by interfering laser beams. The trapped particles can either be larger or smaller than the wavelength. The case that is the closest to the acoustic setup we consider here is that of particles that are smaller than the wavelength (Rayleigh regime). For example the net optical forces acting on non-absorbing dielectric particles that are much smaller than the wavelength, can also be written as the gradient of a potential similar to (1.3) with $\mathfrak{b} = 0$, see e.g. [19,20] and [21] for an explicit comparison of radiation pressure in acoustics and optics. A rigorous treatment of how the theoretical results we present here apply to optical trapping is left for future studies.

Some of the $2-$ and $3-$dimensional crystallographic symmetries that can be achieved using lasers have already been explored in, e.g. [22–27]. To the best of our knowledge, there is no complete characterization of the possible geometries like the one we consider for acoustic trapping. We point out in particular that the study in [26] claims that all 14 Bravais lattices in $3-$dimensions can be realized using 4 lasers. This would seem to be a more general result than the one we present in section 3. Notice however that the linear combinations of plane waves that are proposed in [26] to realize the 14 possible Bravais lattices are not periodic in general, and thus cannot be accurately described as Bravais lattices.

(b) Spatially periodic acoustic waves

To get a periodic arrangement of particles we take the pressure field p to be periodic. This can be achieved by taking a superposition of plane waves with wavevectors $\boldsymbol{k}_1, \ldots, \boldsymbol{k}_d$ in dimension d, that is

$$p(\boldsymbol{x}; \boldsymbol{u}) = \sum_{j=1}^{d} \alpha_j \exp[i\boldsymbol{k}_j \cdot \boldsymbol{x}] + \beta_j \exp[-i\boldsymbol{k}_j \cdot \boldsymbol{x}], \tag{1.4}$$

where $\boldsymbol{u} = [\alpha_1, \ldots, \alpha_d, \beta_1, \ldots, \beta_d]^T$ are complex amplitudes, the wavenumber is $k = |\boldsymbol{k}_j| = 2\pi/\ell$ and the wavelength is $\ell = c/f$. If the wavevectors $\boldsymbol{k}_j$ form a basis of $\mathbb{R}^d$, which is assumed hereinafter, we can define the *lattice* [28] vectors $\boldsymbol{a}_1, \cdots, \boldsymbol{a}_d$ through the relations

$$\boldsymbol{a}_i \cdot \boldsymbol{k}_j = 2\pi\delta_{ij}, \ i, j = 1, \ldots, d. \tag{1.5}$$

Here δ_{ij} is the Kronecker delta with $\delta_{ij} = 1$ if $i = j$ and 0 otherwise. The relation between the lattice vectors and the wavevectors can be written concisely by introducing the $d \times d$ real matrices

[2] Recall that if $\widetilde{\boldsymbol{f}}(t) = \Re(\boldsymbol{f} \exp[-i\omega t])$, then its time average is $\langle|\widetilde{\boldsymbol{f}}(t)|^2\rangle = |\boldsymbol{f}|^2/2$.

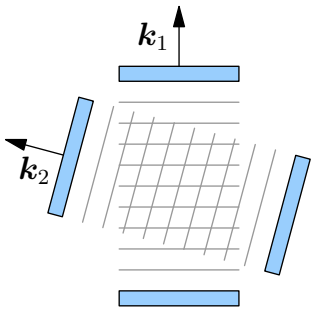

Figure 1. A possible arrangement of ultrasound transducers (in blue) to generate fields close to (1.4) in two dimensions.

$\mathsf{A} \equiv [\boldsymbol{a}_1, \cdots, \boldsymbol{a}_d]$ and $\mathsf{K} \equiv [\boldsymbol{k}_1, \cdots, \boldsymbol{k}_d]$ which should be related by

$$\mathsf{A} = 2\pi \mathsf{K}^{-T}. \tag{1.6}$$

The field p is $\mathsf{A}-$periodic since[3]

$$p(\boldsymbol{x} + \mathsf{A}\boldsymbol{n}; \boldsymbol{u}) = p(\boldsymbol{x}; \boldsymbol{u}) \text{ for any } \boldsymbol{x} \in \mathbb{R}^d,\ \boldsymbol{n} \in \mathbb{Z}^d, \text{ and } \boldsymbol{u} \in \mathbb{C}^{2d}. \tag{1.7}$$

Experimentally we expect that an acoustic pressure field similar to the real part of (1.4) can be obtained far away from planar ultrasound transducers with normal orientations $\boldsymbol{k}_j$ by using the complex amplitudes $\boldsymbol{u}$ to determine the amplitudes and phases of the voltage driving the transducers (see fig. 1 for an illustration). Because of this we call $\boldsymbol{u}$ *transducer parameters*. We do not include the relation between $\boldsymbol{u}$ and an actual transducer's operating voltages as it is out of the scope of the present study.

Remark 1.3. We emphasize that our study is limited to d plane wave directions in dimension d, as this guarantees that the resulting acoustic fields are periodic. Having $n > d$ plane wave directions could break the periodicity and so we can no longer use $2-$ or $3-$dimensional crystallographic symmetries (or Bravais lattices) to describe the possible particle arrangements. Similarly, if we take the restriction to a plane of a $3-$dimensional periodic acoustic field, we may get a field that is not periodic. For example, take wavevectors $\boldsymbol{k}_1 = [\sqrt{2}, 0, \sqrt{10}]^T$, $\boldsymbol{k}_2 = [0, \sqrt{3}, 3]^T$ and $\boldsymbol{k}_3 = [\sqrt{5}, \sqrt{7}, 0]^T$ which have identical length equal to $2\sqrt{3}$. The restriction to the plane $x_3 = 0$ of the field $p(\boldsymbol{x}) = \exp[i\boldsymbol{k}_1 \cdot \boldsymbol{x}] + \exp[i\boldsymbol{k}_2 \cdot \boldsymbol{x}] + \exp[i\boldsymbol{k}_3 \cdot \boldsymbol{x}]$ is not periodic, even if $p(\boldsymbol{x})$ itself is periodic in $\mathbb{R}^3$. This is because the numbers $\sqrt{2}$, $\sqrt{3}$, $\sqrt{5}$ and $\sqrt{7}$ are rationally independent [29] which makes the functions $f(t) = u(t\boldsymbol{v}_0)$ quasi-periodic [30] in t for any non-zero choice of the vector $\boldsymbol{v}_0$. We recall that the numbers $\alpha_1, \ldots, \alpha_n$ are said to be *rationally independent* if the only rational coefficients $\omega_1, \ldots, \omega_n$ for which $\omega_1\alpha_1 + \cdots + \omega_n\alpha_n = 0$ are $\omega_1 = \cdots = \omega_n = 0$.

Since p is $\mathsf{A}-$periodic, its associated acoustic radiation potential ψ must also be $\mathsf{A}-$periodic. In section 2 we show that the extrema of the acoustic radiation potential can be predicted by the maximum and minimum eigenvalues of a $2d \times 2d$ real symmetric matrix. We show that the level-sets of the acoustic radiation potential at values equal to the eigenvalues of this matrix are determined by the associated eigenspace. Note that the relation between the acoustic radiation potential and an eigendecomposition was already exploited in [1,2] to minimize the acoustic radiation potential at a set of points. Here we are in a special case where we can find the minimizers *explicitly* and we give sufficient conditions for these to be isolated points, lines or planes arranged $\mathsf{A}-$periodically. The lattice vectors of the possible particle patterns must have reciprocal vectors with the same length. This limits the possible classes of crystallographic symmetries (Bravais lattices) that can be achieved with this method. We explore this limitation in

[3] We use $\mathbb{R}$ for the real numbers, $\mathbb{C}$ for the complex numbers and $\mathbb{Z} = \{\ldots, -1, 0, 1, \ldots\}$ for the integers.

two and three dimensions in section 3. We summarize our findings and questions that were left open in section 4.

2. Study of the acoustic radiation potential

The key to our study is to write the acoustic radiation potential as a quadratic form of the amplitudes $\boldsymbol{u}$ driving the plane waves (section (a)). We observe that spatial shifts are equivalent to a similarity transformation of the matrix defining the quadratic form. Therefore it suffices to study the acoustic radiation potential at the origin (section (b)), where we can write the eigendecomposition of the associated matrix explicitly. Its eigenvalues give simple bounds on the acoustic radiation potential at constant power. In particular the global minimum values must correspond to the smallest eigenvalue of the associated matrix (section (c)). Then in section (d) we study the possible level-sets of the acoustic radiation potential (at constant power) that are equal to one of the eigenvalues of the associated matrix. These particular level-sets may be composed of lattices (with anywhere between 2 and 2^d points per primitive cell), lines or planes, as is summarized in theorem 2.1.

(a) The acoustic radiation potential as a quadratic form

For a superposition of plane waves of the form (1.4), the acoustic radiation potential at a point $\boldsymbol{x}$ can be written as

$$\psi(\boldsymbol{x};\boldsymbol{u}) = \boldsymbol{u}^* \mathsf{Q}(\boldsymbol{x}) \boldsymbol{u}, \tag{2.1}$$

where the $2d \times 2d$ Hermitian matrix $\mathsf{Q}(\boldsymbol{x})$ is defined by

$$\mathsf{Q}(\boldsymbol{x}) = \mathsf{M}(\boldsymbol{x})^* \begin{bmatrix} \mathfrak{a} & \\ & -\mathfrak{b}\mathsf{I}_d \end{bmatrix} \mathsf{M}(\boldsymbol{x}), \tag{2.2}$$

and we have used the $(d+1) \times 2d$ complex matrix $\mathsf{M}(\boldsymbol{x})$ that is given by

$$\mathsf{M}(\boldsymbol{x}) = [\mathsf{M}_+(\boldsymbol{x})\, \mathsf{M}_-(\boldsymbol{x})] \text{ and } \mathsf{M}_\pm(\boldsymbol{x}) = \begin{bmatrix} \exp[\pm i \boldsymbol{x}^T \mathsf{K}] \\ \mathsf{K}\, \mathrm{diag}(\pm i \exp[\pm i \boldsymbol{x}^T \mathsf{K}]) \end{bmatrix}, \tag{2.3}$$

where the exponential of a vector is understood componentwise and $\mathrm{diag}([a_1, \ldots, a_n])$ is the matrix with diagonal elements $a_1, \ldots, a_n$.

We remark that a translation in $\boldsymbol{x}$ is equivalent to a *unitary* similarity transformation of $\mathsf{Q}(\boldsymbol{x})$. To see this consider a point $\boldsymbol{x} \in \mathbb{R}^d$, and write $\boldsymbol{x} = \boldsymbol{x}_0 + \boldsymbol{\varepsilon}$. Notice that

$$\psi(\boldsymbol{x}_0 + \boldsymbol{\varepsilon}; \boldsymbol{u}) = \psi(\boldsymbol{x}_0; \exp[i[\mathsf{K}, -\mathsf{K}]^T \boldsymbol{\varepsilon}] \odot \boldsymbol{u}), \tag{2.4}$$

where $\odot$ is the componentwise or Hadamard product of two vectors. Indeed, write[4] $\boldsymbol{u} = [\boldsymbol{\alpha}; \boldsymbol{\beta}]$, $\boldsymbol{\alpha}, \boldsymbol{\beta} \in \mathbb{C}^d$, and observe that a spatial shift $\boldsymbol{\varepsilon}$ is equivalent to changing the phase of α_j by $\boldsymbol{k}_j \cdot \boldsymbol{\varepsilon}$ and of β_j by $-\boldsymbol{k}_j \cdot \boldsymbol{\varepsilon}$. Therefore $\mathsf{Q}(\boldsymbol{x}_0 + \boldsymbol{\varepsilon})$ and $\mathsf{Q}(\boldsymbol{x}_0)$ are related by the similarity transformation

$$\mathsf{Q}(\boldsymbol{x}_0 + \boldsymbol{\varepsilon}) = \mathrm{diag}(\exp[i[\mathsf{K}, -\mathsf{K}]^T \boldsymbol{\varepsilon}])^* \mathsf{Q}(\boldsymbol{x}_0)\, \mathrm{diag}(\exp[i[\mathsf{K}, -\mathsf{K}]^T \boldsymbol{\varepsilon}]). \tag{2.5}$$

A practical consequence of (2.5) is that we can study the acoustic radiation potential at a particular point $\boldsymbol{x}_0$ and use (2.4) or (2.5) to deduce its behaviour everywhere else. For simplicity we take $\boldsymbol{x}_0 = \boldsymbol{0}$.

[4] We use semicolons to stack vectors i.e. $[\boldsymbol{\alpha}; \boldsymbol{\beta}] \equiv [\boldsymbol{\alpha}^T, \boldsymbol{\beta}^T]^T$, for vectors $\boldsymbol{\alpha}, \boldsymbol{\beta}$.

(b) The acoustic radiation potential at the origin

Setting $\boldsymbol{x} = \mathbf{0}$ in (2.2) we get that

$$\mathsf{Q}(\mathbf{0}) = \mathfrak{a}\mathbf{1}\mathbf{1}^T - \mathfrak{b}\begin{bmatrix}\mathsf{K}\\ -\mathsf{K}\end{bmatrix}\begin{bmatrix}\mathsf{K}\\ -\mathsf{K}\end{bmatrix}^T, \tag{2.6}$$

where $\mathbf{1}$ is a vector of all ones of appropriate dimension. The following lemma 2.1 gives the eigendecomposition of $\mathsf{Q}(\mathbf{0})$ explicitly in terms of that of $\mathsf{K}\mathsf{K}^T$.

Lemma 2.1. *Let $\sigma_1 \geq \sigma_2 \geq \ldots \geq \sigma_d > 0$ be the eigenvalues of $\mathsf{K}\mathsf{K}^T$ sorted in decreasing order and including multiplicity, and let $\{\boldsymbol{u}_1, \ldots, \boldsymbol{u}_d\}$ be a corresponding real orthonormal basis of eigenvectors*[5]*. Let $\{\boldsymbol{z}_1, \ldots, \boldsymbol{z}_{d-1}\}$ be a real orthonormal basis for $\mathbf{1}^\perp$, the space of vectors orthogonal to $\mathbf{1}$. Then $\mathsf{Q}(\mathbf{0})$ admits the eigendecomposition $\mathsf{Q}(\mathbf{0}) = \mathsf{U}\Lambda\mathsf{U}^T$, where Λ is the $2d \times 2d$ diagonal matrix*

$$\Lambda = \mathrm{diag}([2\mathfrak{a}d, 0, \ldots, 0, -2\mathfrak{b}\sigma_1, \ldots, -2\mathfrak{b}\sigma_d]), \tag{2.7}$$

and U is the real $2d \times 2d$ orthonormal matrix

$$\mathsf{U} = \frac{1}{\sqrt{2}}\begin{bmatrix}\mathbf{1}/\sqrt{d} & \boldsymbol{z}_1 & \ldots & \boldsymbol{z}_{d-1} & \boldsymbol{u}_1 & \ldots & \boldsymbol{u}_d\\ \mathbf{1}/\sqrt{d} & \boldsymbol{z}_1 & \ldots & \boldsymbol{z}_{d-1} & -\boldsymbol{u}_1 & \ldots & -\boldsymbol{u}_d\end{bmatrix}. \tag{2.8}$$

Before proceeding to the proof of lemma 2.1, it is useful to introduce the decomposition $\mathbb{C}^{2d} = H_+ \oplus H_-$ where $H_\pm = \{[\boldsymbol{\alpha}; \pm\boldsymbol{\alpha}] \mid \boldsymbol{\alpha} \in \mathbb{C}^d\}$. The unitary matrices

$$\mathsf{V}_\pm = \frac{1}{\sqrt{2}}\begin{bmatrix}\mathsf{I}_d\\ \pm\mathsf{I}_d\end{bmatrix} \tag{2.9}$$

are such that $H_\pm = \mathrm{range}(\mathsf{V}_\pm)$. Orthogonal projectors onto $H_\pm$ are given by $\mathsf{P}_\pm = \mathsf{V}_\pm\mathsf{V}_\pm^T$.

Proof. From our assumption that the wavevectors $\boldsymbol{k}_1, \ldots, \boldsymbol{k}_d$ form a basis, we deduce that the smallest eigenvalue of $\mathsf{K}\mathsf{K}^T$ should be positive. Indeed if $\boldsymbol{u}$ were a $0-$eigenvector of $\mathsf{K}^T\mathsf{K}$, we would get $0 = \boldsymbol{u}^T\mathsf{K}^T\mathsf{K}\boldsymbol{u} = |\mathsf{K}\boldsymbol{u}|^2$. Since K is invertible, we get the contradiction $\boldsymbol{u} = \mathbf{0}$. Now notice that we have

$$\begin{bmatrix}\mathsf{V}_+\mathsf{V}_-\end{bmatrix}^T \mathsf{Q}(\mathbf{0}) \begin{bmatrix}\mathsf{V}_+\mathsf{V}_-\end{bmatrix} = \begin{bmatrix}2\mathfrak{a}\mathbf{1}\mathbf{1}^T & \\ & -2\mathfrak{b}\mathsf{K}\mathsf{K}^T\end{bmatrix}. \tag{2.10}$$

The eigendecomposition of the matrix on the right-hand side of (2.10) can be obtained from that of $\mathbf{1}\mathbf{1}^T$ and $\mathsf{K}\mathsf{K}^T$. To get the eigendecomposition of $\mathsf{Q}(\mathbf{0})$ from that of the right-hand side of (2.10), it is enough to solve for $\mathsf{Q}(\mathbf{0})$ using that $[\mathsf{V}_+\mathsf{V}_-]$ is an orthonormal matrix. □

(c) Bounds on the acoustic radiation potential

A simple consequence of the acoustic radiation potential being a quadratic form (2.1) is that for any transducer parameters $\boldsymbol{u} \in \mathbb{C}^{2d}$ and positions $\boldsymbol{x} \in \mathbb{R}^d$, we have the bounds

$$\lambda_{\min}(\boldsymbol{x})|\boldsymbol{u}|^2 \leq \psi(\boldsymbol{x}; \boldsymbol{u}) \leq \lambda_{\max}(\boldsymbol{x})|\boldsymbol{u}|^2, \tag{2.11}$$

where $\lambda_{\max,\min}(\boldsymbol{x}) = \lambda_{\max,\min}(\mathsf{Q}(\boldsymbol{x}))$ are the maximum and minimum eigenvalues of $\mathsf{Q}(\boldsymbol{x})$. However we observed in (2.5) that for arbitrary $\boldsymbol{x}$, $\mathsf{Q}(\boldsymbol{x})$ is unitarily similar to $\mathsf{Q}(\mathbf{0})$, thus the eigenvalues of $\mathsf{Q}(\boldsymbol{x})$ do not depend on $\boldsymbol{x}$. By using $\lambda_{\min}(\boldsymbol{x}) = \lambda_{\min}(\mathbf{0})$ and $\lambda_{\max}(\boldsymbol{x}) = \lambda_{\max}(\mathbf{0})$ in (2.11) we get the bound

$$\lambda_{\min}(\mathbf{0})|\boldsymbol{u}|^2 \leq \psi(\boldsymbol{x}; \boldsymbol{u}) \leq \lambda_{\max}(\mathbf{0})|\boldsymbol{u}|^2, \tag{2.12}$$

for any $\boldsymbol{x} \in \mathbb{R}^d$ and $\boldsymbol{u} \in \mathbb{C}^{2d}$. Thus we can achieve the smallest possible acoustic radiation potential at a particular position $\boldsymbol{x}_0$ by choosing transducer parameters $\boldsymbol{u}_{\min}$ within the eigenspace

[5] Alternatively, the σ_j are the squares of the singular values of K and the $\boldsymbol{u}_j$ are its right singular vectors.

of $\mathsf{Q}(\boldsymbol{x}_0)$ corresponding to $\lambda_{\min}(\mathbf{0}) = \lambda_{\min}(\boldsymbol{x}_0)$. Hence $\boldsymbol{u}_{\min}$ gives an explicit solution to the minimization

$$\min_{|\boldsymbol{u}|^2=1} \psi(\boldsymbol{x}_0; \boldsymbol{u}), \tag{2.13}$$

as was remarked in [1,2]. Since the power to generate the plane waves (1.4) is proportional to $|\boldsymbol{u}|^2$, the constraint in (2.13) means that we look only for transducer parameters that require the same power. The bound (2.12) guarantees that with transducer parameters $\boldsymbol{u}_{\min}$, $\boldsymbol{x}_0$ is a global minimum of $\psi(\boldsymbol{x}; \boldsymbol{u}_{\min})$, as a function of $\boldsymbol{x}$. Notice that this choice does not rule out the existence of local minima of $\psi(\boldsymbol{x}; \boldsymbol{u}_{\min})$, where the particles could also be trapped. Also because $\psi(\boldsymbol{x}; \boldsymbol{u}_{\min})$ is $\mathsf{A}-$periodic in $\boldsymbol{x}$, the potential $\psi(\boldsymbol{x}; \boldsymbol{u}_{\min})$ must also have global minima for $\boldsymbol{x}$ on the lattice

$$\{\boldsymbol{x}_0 + \mathsf{A}\boldsymbol{n} \mid \boldsymbol{n} \in \mathbb{Z}^d\}. \tag{2.14}$$

A natural question is whether the global minima are limited to this lattice. This is answered negatively in the next section.

(d) Level-sets of the acoustic radiation potential

The set of all positions $\boldsymbol{x}$ for which the acoustic radiation potential has the same value γ is

$$L_{\gamma,\boldsymbol{u}} = \{\boldsymbol{x} \in \mathbb{R}^d \mid \psi(\boldsymbol{x}; \boldsymbol{u}) = \gamma\}, \tag{2.15}$$

for particular transducer parameters $\boldsymbol{u}$. To simplify the exposition we restrict ourselves to the case $|\boldsymbol{u}| = 1$, i.e. constant power. From the bound (2.12) we see that taking $\boldsymbol{u}$ to be an eigenvector of $\mathsf{Q}(\mathbf{0})$ associated with $\lambda_{\min}(\mathsf{Q}(\mathbf{0}))$ guarantees that the acoustic radiation potential has a global minimum at the origin. In fact the level-sets associated with any eigenpair of $\mathsf{Q}(\mathbf{0})$ are determined by the associated eigenspace.

Lemma 2.2. *Let $\lambda, \boldsymbol{u}$ be an eigenpair of $\mathsf{Q}(\mathbf{0})$ with $|\boldsymbol{u}| = 1$. Then*

$$L_{\lambda,\boldsymbol{u}} = \{\boldsymbol{x} \in \mathbb{R}^d \mid \exp[i[\mathsf{K}, -\mathsf{K}]^T \boldsymbol{x}] \odot \boldsymbol{u} \in \lambda - \textit{eigenspace of } \mathsf{Q}(\mathbf{0})\}.$$

Proof. Let $\boldsymbol{x}$ such that $\exp[i[\mathsf{K}, -\mathsf{K}]^T \boldsymbol{x}] \odot \boldsymbol{u} \in \lambda-$eigenspace of $\mathsf{Q}(\mathbf{0})$. Then from (2.4) and (2.1), we see that $\psi(\boldsymbol{x}; \boldsymbol{u}) = \psi(\mathbf{0}; \exp[i[\mathsf{K}, -\mathsf{K}]^T \boldsymbol{x}] \odot \boldsymbol{u}) = \lambda$. On the other hand if $\boldsymbol{x} \in L_{\lambda,\boldsymbol{u}}$ then $\exp[i[\mathsf{K}, -\mathsf{K}]^T \boldsymbol{x}] \odot \boldsymbol{u}$ must be a $\lambda-$eigenvector of $\mathsf{Q}(\mathbf{0})$. This is because the Rayleigh quotient of a Hermitian matrix is equal to an eigenvalue if and only if it is evaluated at one of the corresponding eigenvectors. □

Notice that by lemma 2.1, we may always be able to pick a $\lambda-$eigenvector of $\mathsf{Q}(\mathbf{0})$ that is of the form $\boldsymbol{u} = [\boldsymbol{v}; \pm\boldsymbol{v}]$, where $|\boldsymbol{v}| = 1/\sqrt{2}$. We now give conditions on the symmetries of the $\lambda-$eigenspace that allow us to decide whether the periodic patterns consist of points, lines or planes. The conditions boil down to checking whether the $\lambda-$eigenvector $\boldsymbol{u}$ remains a $\lambda-$eigenvector after certain sign changes. The results are summarized in the following theorem. We emphasize that the results in theorem 2.1 do not only apply to the global minimum level-sets of the acoustic radiation potential but also to the level-sets corresponding to the other eigenvalues of $\mathsf{Q}(\mathbf{0})$. Nevertheless our results do not say anything about local minima different from the global ones.

Theorem 2.1. *Let $\lambda, \boldsymbol{u}$ be an eigenpair of $\mathsf{Q}(\mathbf{0})$ with $\boldsymbol{u}$ real and $|\boldsymbol{u}| = 1$. Then the acoustic radiation potential level-set $L_{\lambda,\boldsymbol{u}}$ satisfies the following.*

- *If any of the entries of $\boldsymbol{u}$ is zero, then the $\lambda-$level-set of the acoustic radiation potential contains lines or even planes (lemma 2.3). This corresponds to turning off one or more of the transducers.*
- *If $\boldsymbol{u}$ has no zero entries and the $\lambda-$eigenspace of $\mathsf{Q}(\mathbf{0})$ is all contained within either H_+ or H_- then the $\lambda-$level-set of the acoustic radiation potential is composed of between 2 and 2^d isolated*

points per primitive cell (lemma 2.4). The precise number of points is equal to the number of sign changes of $\boldsymbol{u}$ for which the resulting vectors remain in the $\lambda-$eigenspace.

- *If $\boldsymbol{u}$ has no zero entries and the $\lambda-$eigenspace of $\mathsf{Q}(\mathbf{0})$ straddles H_+ and H_- then, the $\lambda-$level-set of the acoustic radiation potential may contain lines (lemma 2.5) or even planes (lemma 2.6).*

The first result applies to the situation where one or more of the transducers is off, i.e. when we pick eigenvectors $\boldsymbol{u}$ that have zero entries in the $\lambda-$eigenspace of $\mathsf{Q}(\mathbf{0})$. In this case, the level-set $L_{\lambda,\boldsymbol{u}}$ contains subspaces of the lattice vectors, which could be either lines or planes, depending on the dimension d.

Lemma 2.3. *Let $\boldsymbol{u} = [\boldsymbol{v}; \pm\boldsymbol{v}]$ be a real unit norm eigenvector of $\mathsf{Q}(\mathbf{0})$ associated with eigenvalue λ. Let $Z = \{j \mid v_j = 0\}$. If any entry of $\boldsymbol{v}$ is zero, i.e. $Z \neq \emptyset$ then*

$$\{\boldsymbol{k}_j \mid j \notin Z\}^{\perp} = \operatorname{span}\{\boldsymbol{a}_j \mid j \in Z\} \subset L_{\lambda,\boldsymbol{u}}. \tag{2.16}$$

Thus the $\lambda-$level-set of the acoustic radiation potential with parameters $\boldsymbol{u}$ must contain any linear combination of the lattice vectors associated with the zero entries in $\boldsymbol{v}$.

Proof. Let $\boldsymbol{z} \in \{\boldsymbol{k}_j \mid j \notin Z\}^{\perp}$, then for $j \notin Z$, $\boldsymbol{k}_j \cdot \boldsymbol{z} = 0$. Or in other words for $j \notin Z$ we have $(\exp[i\mathsf{K}^T\boldsymbol{z}])_j = 1$. Hence we must have that $\exp[i\mathsf{K}^T\boldsymbol{z}] \odot \boldsymbol{v} = \boldsymbol{v}$ since

$$(\exp[i\mathsf{K}^T\boldsymbol{z}])_j v_j = \begin{cases} 0 & \text{for } j \in Z \text{ and} \\ v_j & \text{for } j \notin Z. \end{cases}$$

We conclude that $\exp[i[\mathsf{K}, -\mathsf{K}]^T\boldsymbol{z}] \odot [\boldsymbol{v}; \pm\boldsymbol{v}] = \boldsymbol{u}$ is still an eigenvector of $\mathsf{Q}(\mathbf{0})$ associated with λ and $\psi(\boldsymbol{z}; \boldsymbol{u}) = \psi(\mathbf{0}; \boldsymbol{u}) = \lambda$ by lemma 2.2. The expression in terms of the $\boldsymbol{a}_j$ follows from (1.6). □

When all the entries of the eigenvector $\boldsymbol{u}$ in the $\lambda-$eigenspace of $Q(\mathbf{0})$ are non-zero (i.e. all the transducers are activated), we can guarantee that the level-set $L_{\lambda,\boldsymbol{u}}$ is reduced to up to 2^d points per primitive cell, where the number of points is determined by whether upon changing the signs of the entries of $\boldsymbol{u}$, the new vector remains in the $\lambda-$eigenspace of $Q(\mathbf{0})$.

Lemma 2.4. *Let $\boldsymbol{u} = [\boldsymbol{v}; \pm\boldsymbol{v}] \in H_{\pm}$ be a real unit norm eigenvector of $\mathsf{Q}(\mathbf{0})$ associated with eigenvalue λ, such that $v_j \neq 0$ for all $j = 1, \ldots, d$. Assume that the eigenspace associated with λ is a subset of $H_{\pm}$. Consider the set*[6]

$$T_{\lambda,\boldsymbol{u}} = \{\boldsymbol{s} \in \{0,1\}^d \mid [(-1)^{\boldsymbol{s}} \odot \boldsymbol{v}; \pm(-1)^{\boldsymbol{s}} \odot \boldsymbol{v}] \in \lambda\text{–eigenspace of } \mathsf{Q}(\mathbf{0})\}, \tag{2.17}$$

where $(-1)^{\boldsymbol{s}} \equiv [(-1)^{s_1}, \ldots, (-1)^{s_d}]$. Then $L_{\lambda,\boldsymbol{u}}$ is a union of lattices given by

$$L_{\lambda,\boldsymbol{u}} = \bigcup_{\boldsymbol{s} \in T_{\lambda,\boldsymbol{u}}} \{\boldsymbol{x}(\boldsymbol{n}; \boldsymbol{s}) = \mathsf{A}(\boldsymbol{n} + \boldsymbol{s}/2) \mid \boldsymbol{n} \in \mathbb{Z}^d\}. \tag{2.18}$$

Proof. We would like to show that $\psi(\boldsymbol{x}; \boldsymbol{u}) = \psi(\mathbf{0}; \boldsymbol{u}) = \lambda$ if and only if $\boldsymbol{x}$ belongs to one of the lattices in (2.18).

Let us first assume that $\boldsymbol{x}$ belongs to one of the lattices in (2.18). Then we can find $\boldsymbol{s} \in \{0,1\}^d$ such that $[(-1)^{\boldsymbol{s}}\boldsymbol{v}; \pm(-1)^{\boldsymbol{s}}\boldsymbol{v}]$ is in the $\lambda-$eigenspace of $\mathsf{Q}(\mathbf{0})$ and $\boldsymbol{x} = \mathsf{A}(\boldsymbol{n} + \boldsymbol{s}/2)$ for some $\boldsymbol{n} \in \mathbb{Z}^d$.

[6]The set $T_{\lambda,\boldsymbol{u}}$ is never empty since $\{\mathbf{0}, \mathbf{1}\} \subset T_{\lambda,\boldsymbol{u}}$, because the vectors $\pm\boldsymbol{u}$ always belong to the same subspace.

By (1.6) we have that $\exp[i\boldsymbol{k}_j \cdot \boldsymbol{x}] = \exp[i2\pi(n_j + s_j/2)] = (-1)^{s_j}$ and so we also have

$$\exp[i[\mathsf{K}, -\mathsf{K}]^T \boldsymbol{x}] = \exp[-i[\mathsf{K}, -\mathsf{K}]^T \boldsymbol{x}] = [(-1)^{\boldsymbol{s}}; (-1)^{\boldsymbol{s}}]. \tag{2.19}$$

We conclude that the vector $\exp[i[\mathsf{K}, -\mathsf{K}]^T \boldsymbol{x}] \odot [\boldsymbol{v}; \pm\boldsymbol{v}]$ belongs to the $\lambda-$eigenspace of $\mathsf{Q}(\boldsymbol{0})$. In other words, $\boldsymbol{x} \in L_{\lambda,\boldsymbol{u}}$ since by (2.4) we have

$$\psi(\boldsymbol{x}; \boldsymbol{u}) = \psi(\boldsymbol{0}; \exp[i[\mathsf{K}, -\mathsf{K}]^T \boldsymbol{x}] \odot [\boldsymbol{v}; \pm\boldsymbol{v}]) = \psi(\boldsymbol{0}; \boldsymbol{u}) = \lambda.$$

Now let us assume that $\boldsymbol{x} \in L_{\boldsymbol{u},\lambda}$, i.e. $\psi(\boldsymbol{x}; \boldsymbol{u}) = \lambda$. By using (2.4) again we have that $\exp[i[\mathsf{K}, -\mathsf{K}]^T \boldsymbol{x}] \odot [\boldsymbol{v}; \pm\boldsymbol{v}]$ must be in the $\lambda-$eigenspace of $\mathsf{Q}(\boldsymbol{0})$. Moreover the former vector can be split into components in $H_\pm$ and $H_\mp$ as follows

$$\exp\left[i\begin{bmatrix}\mathsf{K}^T\\ -\mathsf{K}^T\end{bmatrix}\boldsymbol{x}\right] \odot \begin{bmatrix}\boldsymbol{v}\\ \pm\boldsymbol{v}\end{bmatrix} = \underbrace{\cos\left[\begin{bmatrix}\mathsf{K}^T\\ -\mathsf{K}^T\end{bmatrix}\boldsymbol{x}\right] \odot \begin{bmatrix}\boldsymbol{v}\\ \pm\boldsymbol{v}\end{bmatrix}}_{\in H_\pm} + i\underbrace{\sin\left[\begin{bmatrix}\mathsf{K}^T\\ -\mathsf{K}^T\end{bmatrix}\boldsymbol{x}\right] \odot \begin{bmatrix}\boldsymbol{v}\\ \pm\boldsymbol{v}\end{bmatrix}}_{\in H_\mp}. \tag{2.20}$$

Since we assumed that the $\lambda-$eigenspace of $\mathsf{Q}(\boldsymbol{0})$ is a subspace of $H_\pm$ we must have that $\exp[i[\mathsf{K}, -\mathsf{K}]^T \boldsymbol{x}] \odot [\boldsymbol{v}; \pm\boldsymbol{v}] \in H_\pm$ and its $H_\mp$ component must be zero. By the decomposition (2.20), this means that $\exp[i[\mathsf{K}, -\mathsf{K}]^T \boldsymbol{x}] \odot [\boldsymbol{v}; \pm\boldsymbol{v}]$ must be real. Using the definition (2.17) of the set $T_{\lambda,\boldsymbol{u}}$, we see that there must be an $\boldsymbol{s} \in \{0, 1\}^d$ such that (2.19) holds. This imposes that $\boldsymbol{x}$ must be part of the lattice (2.18) with $\boldsymbol{s} \in T_{\lambda,\boldsymbol{u}}$. □

To better illustrate lemma 2.4, let us define the primitive cell

$$C = \{\mathsf{A}\boldsymbol{\alpha} \mid \boldsymbol{\alpha} \in [0, 1]^d\}. \tag{2.21}$$

Points within the primitive cell can be identified by their "atomic coordinates" $\boldsymbol{\alpha} \in [0, 1]^d$. Thus we have the following extreme cases.

i. If λ is a simple eigenvalue then $T_{\lambda,\boldsymbol{u}} = \{\boldsymbol{0}, \boldsymbol{1}\}$ and there are two points per primitive cell in $L_{\lambda,\boldsymbol{u}}$, namely $\boldsymbol{0}$ and $\boldsymbol{1}/2$, in atomic coordinates, provided $\boldsymbol{u}$ is a unit length eigenvector of $\mathsf{Q}(\boldsymbol{0})$ with non-zero entries.
ii. If λ is an eigenvalue of multiplicity d, then $T_{\lambda,\boldsymbol{u}} = \{0, 1\}^d$ and there are exactly 2^d points in $L_{\lambda,\boldsymbol{u}}$ per primitive cell, namely the points with atomic coordinates $\boldsymbol{s}/2$, where $\boldsymbol{s} \in \{0, 1\}^d$. This is of course provided $\boldsymbol{u}$ is a unit length eigenvector of $\mathsf{Q}(\boldsymbol{0})$ with non-zero entries and the $\lambda-$eigenspace of $\mathsf{Q}(\boldsymbol{0})$ is all within either H_+ or H_-.

Example 2.1 (Eigenvalue of multiplicity 2)**.** Consider a 2D example. Choose the wavevectors so that $\mathsf{K} = \mathsf{I}_2$ and $\ell = 2\pi$. Setting $\mathfrak{a} = \mathfrak{b} = 1$ in the acoustic radiation potential and using (2.6) we get

$$\mathsf{Q}(\boldsymbol{0}) = \boldsymbol{1}\boldsymbol{1}^T - \begin{bmatrix}\mathsf{K}\\ -\mathsf{K}\end{bmatrix}\begin{bmatrix}\mathsf{K}\\ -\mathsf{K}\end{bmatrix}^T = \begin{bmatrix}0 & 1 & 2 & 1\\ 1 & 0 & 1 & 2\\ 2 & 1 & 0 & 1\\ 1 & 2 & 1 & 0\end{bmatrix}. \tag{2.22}$$

We choose the eigendecomposition $\mathsf{Q}(\boldsymbol{0}) = \mathsf{U}\Lambda\mathsf{U}^T$ with

$$\mathsf{U} = \begin{bmatrix}1/2 & -1/2 & 1/\sqrt{2} & 0\\ 1/2 & 1/2 & 0 & 1/\sqrt{2}\\ 1/2 & -1/2 & -1/\sqrt{2} & 0\\ 1/2 & 1/2 & 0 & -1/\sqrt{2}\end{bmatrix}, \tag{2.23}$$

and $\mathrm{diag}(\Lambda) = \{4, 0, -2, -2\}$ such that it conforms to H_+ and H_-, as in lemma 2.1. Notice that the $(-2)-$eigenspace of $\mathsf{Q}(\boldsymbol{0})$ is identical to H_-. Thus a real unit length $(-2)-$eigenvector $\boldsymbol{u}$ with no zero entries must have the form $\boldsymbol{u} = [u_1, u_2, -u_1, -u_2]$. Notice that by changing the sign of u_1 and/or u_2 we get a vector that remains inside H_-. We deduce that $T_{-2,\boldsymbol{u}} = \{0, 1\}^2$ (see lemma 2.4

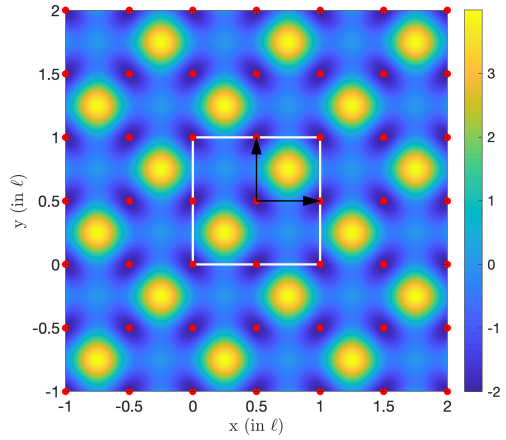

Figure 2. Acoustic radiation potential (from example 2.1) resulting in a tetragonal lattice arrangement of minima when the eigenvector has no zero entries. A primitive cell is outlined in white. The points in the lattice (2.24) are shown in red. Since the minimum eigenvalue of $\mathsf{Q}(\mathbf{0})$ has multiplicity 2, there are 4 minimum points per primitive cell. The black arrows indicate the directions normal to the transducers.

for the definition of this set). Hence lemma 2.4, predicts acoustic radiation potential minima at the union of lattices

$$\bigcup_{\boldsymbol{s}\in\{0,1\}^2} \{\boldsymbol{x}(\boldsymbol{n};\boldsymbol{s}) = 2\pi(\boldsymbol{n}+\boldsymbol{s}/2) \mid \boldsymbol{n}\in\mathbb{Z}^d\}. \tag{2.24}$$

Figure 2 shows that the acoustic radiation potential for this example with eigenvector $\boldsymbol{u} = [1,1,-1,-1]^T/2$ has 4 minimum points per primitive cell.

If we consider the acoustic radiation potential for an eigenvector with zero entries, we no longer have strict minima, by lemma 2.3. This is illustrated in fig. 3, which shows the acoustic radiation potential for the same example, but with eigenvector $\boldsymbol{u} = [1,0,-1,0]^T/\sqrt{2}$.

Lemma 2.5. *Let $\boldsymbol{u} = [\boldsymbol{v};\pm\boldsymbol{v}] \in H_\pm$ be a real unit norm eigenvector of $\mathsf{Q}(\mathbf{0})$ associated with eigenvalue λ. Consider the set $T^{\pm}_{\lambda,\boldsymbol{u}}$ defined by*

$$T^{\pm}_{\lambda,\boldsymbol{u}} = \left\{\boldsymbol{s}\in\{0,1\}^d \mid [(-1)^{\boldsymbol{s}}\odot\boldsymbol{v};\mp(-1)^{\boldsymbol{s}}\odot\boldsymbol{v}] \in \lambda\text{–eigenspace of } \mathsf{Q}(\mathbf{0})\right\}. \tag{2.25}$$

Notice that if the set $T^{\pm}_{\lambda,\boldsymbol{u}}$ is not empty, the $\lambda-$eigenspace of $\mathsf{Q}(\mathbf{0})$ straddles between H_+ and H_-, which is a possibility predicted by lemma 2.1. Then we can guarantee that $L_{\lambda,\boldsymbol{u}}$ contains the lines

$$\{\boldsymbol{x}(\boldsymbol{n};\theta) = \mathsf{K}^{-T}(\theta(-1)^{\boldsymbol{s}} + 2\pi\boldsymbol{n}) \mid \theta\in\mathbb{R}\} \text{ for } \boldsymbol{n}\in\mathbb{Z}^d \text{ and } \boldsymbol{s}\in T^{\pm}_{\lambda,\boldsymbol{u}}. \tag{2.26}$$

Proof. Assume that $\boldsymbol{x}$ belongs to one of the lines (2.26), we would like to show that $\psi(\boldsymbol{x};\boldsymbol{u}) = \psi(\mathbf{0};\boldsymbol{u}) = \lambda$. Then $\mathsf{K}^T\boldsymbol{x} = \theta(-1)^{\boldsymbol{s}} + 2\pi\boldsymbol{n}$, and we have that $\exp[i\boldsymbol{k}_j\cdot\boldsymbol{x}] = \exp[i\theta(-1)^{s_j}]$. The following decomposition in terms of a vector in $H_\pm$ and in $H_\mp$ holds

$$\exp\left[i\begin{bmatrix}\mathsf{K}^T\\-\mathsf{K}^T\end{bmatrix}\boldsymbol{x}\right]\odot\begin{bmatrix}\boldsymbol{v}\\\pm\boldsymbol{v}\end{bmatrix} = \cos\theta\begin{bmatrix}\boldsymbol{v}\\\pm\boldsymbol{v}\end{bmatrix} + i\sin\theta\begin{bmatrix}(-1)^{\boldsymbol{s}}\\(-1)^{\boldsymbol{s}}\end{bmatrix}\odot\begin{bmatrix}\boldsymbol{v}\\\mp\boldsymbol{v}\end{bmatrix}. \tag{2.27}$$

By the definition of the set $T^{\pm}_{\lambda,\boldsymbol{u}}$, the vector $[(-1)^{\boldsymbol{s}}\odot\boldsymbol{v};\mp(-1)^{\boldsymbol{s}}\odot\boldsymbol{v}]$ must be a $\lambda-$eigenvector of $\mathsf{Q}(\mathbf{0})$. Hence $\exp[i[\mathsf{K}^T;-\mathsf{K}^T]\boldsymbol{x}]\odot[\boldsymbol{v};\pm\boldsymbol{v}]$ is also a $\lambda-$eigenvector of $\mathsf{Q}(\mathbf{0})$. Thus by (2.4), $\boldsymbol{x}$ remains in the $\lambda-$level-set of ψ, i.e. $\psi(\boldsymbol{x};\boldsymbol{u}) = \lambda$. □

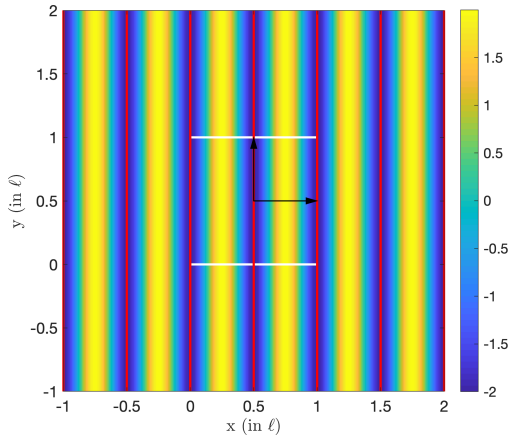

Figure 3. The acoustic radiation potential defined in example 2.1 results in lines of minima if the eigenvector used to compute the acoustic radiation potential has zero entries. The lines where minima lie are the spans of the lattice vectors specified by (2.16) and are indicated in red. A primitive cell is outlined in white. The black arrows indicate the directions normal to the transducers.

Example 2.2 (Lines of minima)**.** Consider a 2D example. Choose the wavevectors so $\mathsf{K} = \mathsf{I}_2$, $\ell = 2\pi$ and set $\mathfrak{a} = 1, \mathfrak{b} = 0$ in the acoustic radiation potential. By (2.6), we have $\mathsf{Q}(\mathbf{0}) = \mathbf{1}\mathbf{1}^T$. We choose the eigendecomposition $\mathsf{Q}(\mathbf{0}) = \mathsf{U}\Lambda\mathsf{U}^T$ with $\mathrm{diag}(\Lambda) = \{4, 0, 0, 0\}$ and

$$\mathsf{U} = \frac{1}{\sqrt{2}} \begin{bmatrix} 1/\sqrt{2} & -1/\sqrt{2} & 1 & 0 \\ 1/\sqrt{2} & 1/\sqrt{2} & 0 & 1 \\ 1/\sqrt{2} & -1/\sqrt{2} & -1 & 0 \\ 1/\sqrt{2} & 1/\sqrt{2} & 0 & -1 \end{bmatrix}. \tag{2.28}$$

This eigendecomposition conforms with H_+ and H_- and is consistent with lemma 2.1. Notice that the $0-$eigenspace of $\mathsf{Q}(\mathbf{0})$ straddles over H_+ and H_-, and that this eigenspace contains all of H_-. The real unit length vector $\boldsymbol{u} = [-1, 1, -1, 1]^T/2$ (the second column of U) belongs to both H_+ and the $0-$eigenspace of $\mathsf{Q}(\mathbf{0})$. Using definition (2.25) we can verify that $T^{\pm}_{0,\boldsymbol{u}} = \{0, 1\}^2$. Thus lemma 2.5 predicts acoustic radiation potential minima along the families of lines

$$\{\boldsymbol{x}(\boldsymbol{n}; \theta) = \mathsf{K}^{-T}(\theta(-1)^{\boldsymbol{s}} + 2\pi\boldsymbol{n}) \mid \theta \in \mathbb{R}\}, \text{ for } \boldsymbol{n} \in \mathbb{Z}^d \text{ and } \boldsymbol{s} \in \{0, 1\}^2. \tag{2.29}$$

These lines are indicated in fig. 4 and coincide with minima of the acoustic radiation potential.

Lemma 2.6. *Let $\boldsymbol{u} = [\boldsymbol{v}; \pm\boldsymbol{v}] \in H_\pm$ be a real unit norm eigenvector of $\mathsf{Q}(\mathbf{0})$ associated with eigenvalue λ. Consider the set $R^{\pm}_{\lambda,\boldsymbol{u}}$ defined by*

$$R^{\pm}_{\lambda,\boldsymbol{u}} = \Bigg\{ (\boldsymbol{s}, \boldsymbol{r}) \in (\{0, 1\}^d)^2 \;\Bigg|\; \begin{bmatrix} (-1)^{\boldsymbol{s}} \\ (-1)^{\boldsymbol{s}} \end{bmatrix} \odot \begin{bmatrix} \boldsymbol{v} \\ \mp\boldsymbol{v} \end{bmatrix}, \begin{bmatrix} (-1)^{\boldsymbol{r}} \\ (-1)^{\boldsymbol{r}} \end{bmatrix} \odot \begin{bmatrix} \boldsymbol{v} \\ \mp\boldsymbol{v} \end{bmatrix}, \begin{bmatrix} (-1)^{\boldsymbol{s}+\boldsymbol{r}} \\ (-1)^{\boldsymbol{s}+\boldsymbol{r}} \end{bmatrix} \odot \begin{bmatrix} \boldsymbol{v} \\ \pm\boldsymbol{v} \end{bmatrix} \in \lambda\text{–eigenspace of } \mathsf{Q}(\mathbf{0}) \Bigg\}. \tag{2.30}$$

Notice that if the set $R^{\pm}_{\lambda,\boldsymbol{u}}$ is not empty, the λ-eigenspace of $\mathsf{Q}(\mathbf{0})$ straddles between H_+ and H_-. Then we can guarantee $L_{\lambda,\boldsymbol{u}}$ contains the sets

$$\{\boldsymbol{x}(\boldsymbol{n}; \theta, \phi) = \mathsf{K}^{-T}(\theta(-1)^{\boldsymbol{s}} + \phi(-1)^{\boldsymbol{r}} + 2\pi\boldsymbol{n}) \mid \theta, \phi \in \mathbb{R}\}, \tag{2.31}$$

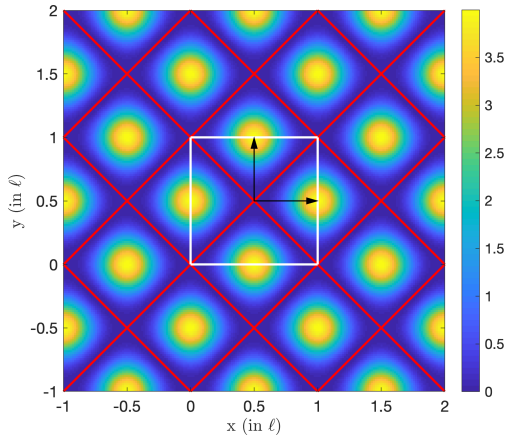

Figure 4. Acoustic radiation potential of example 2.2 resulting in lines of minima. A primitive cell is outlined in white. The lines predicted by (2.29) are shown in red. The black arrows indicate the directions normal to the transducers.

for $\boldsymbol{n} \in \mathbb{Z}^d$ *and* $(\boldsymbol{s}, \boldsymbol{r}) \in R^{\pm}_{\lambda,\boldsymbol{u}}$. *The sets in* (2.31) *are guaranteed to be planes when the vectors* $(-1)^{\boldsymbol{r}}$ *and* $(-1)^{\boldsymbol{s}}$ *are linearly independent or equivalently* $(-1)^{\boldsymbol{r}+\boldsymbol{s}} \notin \{-\mathbf{1}, \mathbf{1}\}$.

Proof. Assume $\boldsymbol{x}$ belongs to one of the planes (2.31), we would like to show that $\psi(\boldsymbol{x}; \boldsymbol{u}) = \psi(\mathbf{0}; \boldsymbol{u}) = \lambda$. Since $\mathsf{K}^T\boldsymbol{x} = \theta(-1)^{\boldsymbol{s}} + \phi(-1)^{\boldsymbol{r}} + 2\pi\boldsymbol{n}$, we must have that $\exp[i\boldsymbol{k}_j \cdot \boldsymbol{x}] = \exp[i(\theta(-1)^{s_j} + \phi(-1)^{r_j})]$. Then we obtain the following decomposition in terms of vectors in $H_{\pm}$ and $H_{\mp}$,

$$\begin{aligned}\exp\left[i\begin{bmatrix}\mathsf{K}^T\\ -\mathsf{K}^T\end{bmatrix}\boldsymbol{x}\right] \odot \begin{bmatrix}\boldsymbol{v}\\ \pm\boldsymbol{v}\end{bmatrix} = &\left(\cos\theta\cos\phi\begin{bmatrix}\mathbf{1}\\ \mathbf{1}\end{bmatrix} - \sin\theta\sin\phi\begin{bmatrix}(-1)^{\boldsymbol{s}+\boldsymbol{r}}\\ (-1)^{\boldsymbol{s}+\boldsymbol{r}}\end{bmatrix}\right) \odot \begin{bmatrix}\boldsymbol{v}\\ \pm\boldsymbol{v}\end{bmatrix}\\ &+i\left(\sin\theta\cos\phi\begin{bmatrix}(-1)^{\boldsymbol{s}}\\ (-1)^{\boldsymbol{s}}\end{bmatrix} + \cos\theta\sin\phi\begin{bmatrix}(-1)^{\boldsymbol{r}}\\ (-1)^{\boldsymbol{r}}\end{bmatrix}\right) \odot \begin{bmatrix}\boldsymbol{v}\\ \mp\boldsymbol{v}\end{bmatrix}.\end{aligned} \tag{2.32}$$

By definition of the set $R^{\pm}_{\lambda,\boldsymbol{u}}$, each vector in the decomposition must be a $\lambda-$eigenvector of $\mathsf{Q}(\mathbf{0})$. Hence $\exp[i[\mathsf{K}^T; -\mathsf{K}^T]\boldsymbol{x}] \odot [\boldsymbol{v}; \pm\boldsymbol{v}]$ is also a λ-eigenvector of $\mathsf{Q}(\mathbf{0})$. By (2.4) this implies that $\psi(\boldsymbol{x}; \boldsymbol{u}) = \lambda$. □

Example 2.3 (Planes of minima)**.** Consider a 3D example. Choose the wavevectors so $\mathsf{K} = \mathsf{I}_3$. Setting $\mathfrak{a} = 1, \mathfrak{b} = 0$ in the acoustic radiation potential gives $\mathsf{Q}(\mathbf{0}) = \mathbf{1}\mathbf{1}^T$. An eigendecomposition $\mathsf{Q}(\mathbf{0}) = \mathsf{U}\Lambda\mathsf{U}^T$ is chosen such that $\mathrm{diag}(\Lambda) = \{6, 0, 0, 0, 0, 0\}$ and

$$\mathsf{U} = \frac{1}{\sqrt{2}}\begin{bmatrix}1/\sqrt{3} & 1/\sqrt{2} & 1/\sqrt{6} & 1 & 0 & 0\\ 1/\sqrt{3} & -1/\sqrt{2} & 1/\sqrt{6} & 0 & 1 & 0\\ 1/\sqrt{3} & 0 & -2/\sqrt{6} & 0 & 0 & 1\\ 1/\sqrt{3} & 1/\sqrt{2} & 1/\sqrt{6} & -1 & 0 & 0\\ 1/\sqrt{3} & -1/\sqrt{2} & 1/\sqrt{6} & 0 & -1 & 0\\ 1/\sqrt{3} & 0 & -2/\sqrt{6} & 0 & 0 & -1\end{bmatrix}, \tag{2.33}$$

conforming to H_+ and H_- (as in lemma 2.1). The $0-$eigenspace of $\mathsf{Q}(\mathbf{0})$ straddles over H_+ and H_-, and contains all of H_-. The real unit length vector $\boldsymbol{u} = [1, -1, 0, 1, -1, 0]^T/2$ (the second column of U) belongs to both H_+ and the $0-$eigenspace of $\mathsf{Q}(\mathbf{0})$. Using definition (2.30) we can verify that

$$R^{\pm}_{0,\boldsymbol{u}} = \left\{(\boldsymbol{s}, \boldsymbol{r}) \in \{0, 1\}^3 \times \{0, 1\}^3 \mid (-1)^{s_1+r_1} = (-1)^{s_2+r_2}\right\}. \tag{2.34}$$

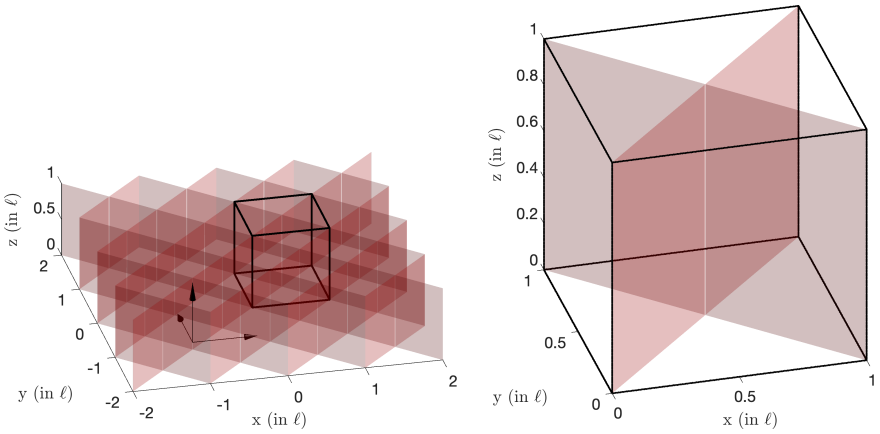

Figure 5. The minima of the acoustic radiation potential defined in example 2.3 appear on planes. The planes are displayed on a few unit cells (left) and for more clarity on a unit cell (right). The black arrows indicate the directions normal to the transducers.

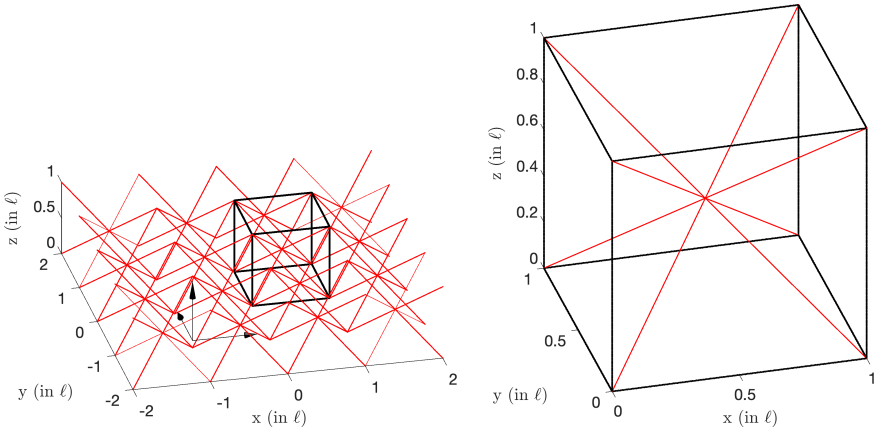

Figure 6. The minima of the acoustic radiation potential in example 2.4 appear on lines. The lines are displayed on a few unit cells (left) and for more clarity on a unit cell (right). The black arrows indicate the directions normal to the transducers.

Thus lemma 2.6 predicts acoustic radiation potential minima along the sets given in eq. (2.31), some of them being the planes indicated in fig. 5. We have verified numerically that they coincide with the minima of the acoustic radiation potential.

Example 2.4. Using the same matrix in (2.33) but choosing the unit-length $0-$eigenvector $\boldsymbol{v} = [1,1,-2,1,1,-2]/2\sqrt{3} \in H_+$ we get

$$R^{\pm}_{0,\boldsymbol{v}} = \left\{ (\boldsymbol{s},\boldsymbol{r}) \in \{0,1\}^3 \times \{0,1\}^3 \mid (-1)^{s_1+r_1} = (-1)^{s_2+r_2} = (-1)^{s_3+r_3} \right\}. \tag{2.35}$$

Now all the corresponding sets in (2.31) are lines because we have that $(-1)^{\boldsymbol{s}+\boldsymbol{r}} \in \{-\mathbf{1},\mathbf{1}\}$ for $(\boldsymbol{s},\boldsymbol{r}) \in R^{\pm}_{0,\boldsymbol{v}}$. These lines are displayed in fig. 6.

3. Achievable Bravais lattice classes

In earlier sections, we have taken the wavevectors $\boldsymbol{k}_1, \ldots, \boldsymbol{k}_d$ to be fixed. Now, we address the question of how to choose these vectors in order to obtain an arrangement of particles on a particular Bravais lattice. The position of the particles is dictated by the acoustic radiation potential $\psi(\boldsymbol{x}; \boldsymbol{u})$ which is $\mathsf{A}-$periodic. Since $\mathsf{A} = 2\pi\mathsf{K}^{-T}$, and all the columns of K have the same length k, there are limitations to the possible Bravais lattices that we can obtain. To explore these limitations, we introduce the following definition.

Definition 3.1. We say that a Bravais lattice class is *achievable* if out of all class members with reciprocal lattice vectors $\boldsymbol{k}_1, \ldots, \boldsymbol{k}_d$ having same length, i.e.

$$|\boldsymbol{k}_1| = \cdots = |\boldsymbol{k}_d| \tag{3.1}$$

there is at least one member that does not belong to any of the other Bravais lattice classes.

In other words, a Bravais lattice class *cannot be achieved* if under the constraint of definition 3.1, all Bravais lattices within a class happen to belong to another class. For a two dimensional example, notice that tetragonal lattices are members of the orthorhombic lattice class. However, when we place the same length constraint on the reciprocal lattice vectors for an orthorhombic lattice, we end up with a tetragonal lattice. Thus we say that the orthorhombic lattice class cannot be achieved. We remark that definition 3.1 is irrespective of the particular particle arrangement inside a primitive cell, which could include isolated points, lines or planes (theorem 2.1).

Our results are summarized in tables 1 and 2 for two and three dimensions, respectively. We found that out of the 5 Bravais lattice classes in two dimensions (see e.g. [28]) only three are achievable. In three dimensions, there are 14 Bravais lattice classes (see e.g. [28]) but we found that only 6 are achievable.

To generate tables 1 and 2, we took known reference tables associating Bravais lattice classes to the typical form of their reciprocal vectors. Then we imposed the condition that all the reciprocal vectors have the same norm[7]. A general form for the reciprocal vectors is given in the second column of these tables. If the third column has an entry, then the particular class cannot be achieved and the class that is implied by the same norm reciprocal vector constraint is indicated. If the third column has no entry, it means that at least one representative belonging exclusively to the class can be achieved. Of course, tables 1 and 2 can be used to design lattices by taking the transducer normal orientations to be those in the second column. The reference tables we based our study on can be found in [31, Table 3.3] for three dimensions. The two dimensional reciprocal vectors can be derived from e.g. [28, Fig. 1.7] and (1.6). We also illustrate in figs. 7 and 8 representatives of the classes of Bravais lattices that are achievable using standing acoustic waves, in the particular case of isolated particle arrangements.

4. Summary and perspectives

We have shown that the behaviour of a periodic acoustic radiation potential in two or three dimensions can be characterized by a 4×4 or 6×6 real symmetric matrix, whose eigendecomposition can be found explicitly. Our main result is to use symmetries of the corresponding eigenspaces to predict whether the global minima of the acoustic radiation potential are limited to points, lines or planes. It is still an open question whether the global minima for periodic acoustic radiation potentials can be more general curves or surfaces. We also identify classes of Bravais lattices that can be achieved using a periodic acoustic radiation potential. We are currently working on extending this work to quasi-periodic arrangements of particles, which correspond to the case where we use a number of transducer directions that is larger than the dimension d. Notice that the acoustic radiation potential derivation assumes

[7] For certain lattices we used reciprocal vectors with norm different from one, in an effort to get simpler expressions.

Bravais lattice class	Reciprocal lattice vectors	Implied symmetry
Monoclinic	$\boldsymbol{g}_1 = (1, -\cot\gamma)$ $\boldsymbol{g}_2 = (0, \csc\gamma)$	Orthorhombic centred
Orthorhombic	$\boldsymbol{g}_1 = (1, 0)$ $\boldsymbol{g}_2 = (0, 1)$	Tetragonal
Orthorhombic centred	$\boldsymbol{g}_1 = (\csc(\gamma)\sin(\gamma/2), \csc(\gamma/2)/2)$ $\boldsymbol{g}_2 = (\csc(\gamma)\sin(\gamma/2), -\csc(\gamma/2)/2)$	
Hexagonal	$\boldsymbol{g}_1 = (1, 1/\sqrt{3})$ $\boldsymbol{g}_2 = (0, 2/\sqrt{3})$	
Tetragonal	$\boldsymbol{g}_1 = (1, 0)$ $\boldsymbol{g}_2 = (0, 1)$	

Table 1. Two dimensional Bravais lattice classes that are achievable using standing acoustic waves. The reciprocal lattice vectors we give satisfy $|\boldsymbol{g}_1| = |\boldsymbol{g}_2|$, so they need to be rescaled so that their length is k in order to be interpreted as the wavevectors needed to obtain a particular Bravais lattice. The angle γ is the angle between the two primitive vectors in the lattice.

the particles are spherical. Thus it is also interesting to see how the particle shape influences the possible periodic arrangements of particles. We also plan to characterize the scattering off gratings for millimetre waves that can be fabricated using ultrasound directed self-assembly.

Data Accessibility. Matlab code for generating figs. 2 to 8 is available at `https://github.com/fguevaravas/crystals` and has been tested with Matlab versions 2014b and 2018b on Mac OS X.

Authors' Contributions. FGV and CM contributed to designing, organizing and proving the theoretical results. The design of the numerical experiments is due to FGV and CM. The numerical experiments were written and performed by CM. Both authors contributed equally to writing and revising the final manuscript.

Funding. The authors acknowledge support from Army Research Office Contract No. W911NF-16-1-0457.

Acknowledgements. The authors would like to thank the anonymous referees for pointing out the possible relation between our work and optical lattices.

References

1. Greenhall J, Guevara Vasquez F, Raeymaekers B. 2016 Ultrasound directed self-assembly of user-specified patterns of nanoparticles dispersed in a fluid medium. *Applied Physics Letters* **108**, 103103.
2. Prisbrey M, Greenhall J, Guevara Vasquez F, Raeymaekers B. 2017 Ultrasound directed self-assembly of three-dimensional user-specified patterns of particles in a fluid medium. *Journal of Applied Physics* **121**, 014302.
3. Friend J, Yeo LY. 2011 Microscale acoustofluidics: Microfluidics driven via acoustics and ultrasonics. *Rev. Mod. Phys.* **83**, 647–704.
4. Wiklund M, Radel S, Hawkes JJ. 2013 Acoustofluidics 21: ultrasound-enhanced immunoassays and particle sensors. *Lab Chip* **13**, 25–39.
5. Meng L, Cai F, Li F, Zhou W, Niu L, Zheng H. 2019 Acoustic tweezers. *Journal of Physics D: Applied Physics* **52**, 273001.
6. Courtney CRP, Demore CEM, Wu H, Grinenko A, Wilcox PD, Cochran S, Drinkwater BW. 2014 Independent trapping and manipulation of microparticles using dexterous acoustic tweezers. *Applied Physics Letters* **104**, 154103.
7. Marzo A, Drinkwater BW. 2019 Holographic acoustic tweezers. *Proceedings of the National Academy of Sciences* **116**, 84–89.
8. Ozcelik A, Rufo J, Guo F, Gu Y, Li P, Lata J, Huang TJ. 2018 Acoustic tweezers for the life sciences. *Nature Methods* **15**, 1021–1028.

Bravais lattice class	Reciprocal lattice vectors	Implied symmetry
Triclinic primitive	$\lvert\boldsymbol{g}_1\rvert = \lvert\boldsymbol{g}_2\rvert = \lvert\boldsymbol{g}_3\rvert$	
Monoclinic primitive	$\boldsymbol{g}_1 = (-\cos\gamma, -\sin\gamma, 0)$ $\boldsymbol{g}_2 = (1, 0, 0)$ $\boldsymbol{g}_3 = (0, 0, 1)$	Cubic primitive (if $\cos\gamma = 0$) Tetragonal body-centred (if $\cos\gamma \neq 0$)
Monoclinic base-centred	$\boldsymbol{g}_1 = (-\cot\gamma, -1, 0)$ $\boldsymbol{g}_2 = \frac{1}{ac}(c\csc\gamma, 0, -a)$ $\boldsymbol{g}_3 = \frac{1}{ac}(c\csc\gamma, 0, a)$	Tetragonal body-centred
Orthorhombic primitive	$\boldsymbol{g}_1 = (0, -1, 0)$ $\boldsymbol{g}_2 = (1, 0, 0)$ $\boldsymbol{g}_3 = (0, 0, 1)$	Cubic primitive
Orthorhombic base-centred	$\boldsymbol{g}_1 = (b, -a, 0)$ $\boldsymbol{g}_2 = (b, a, 0)$ $\boldsymbol{g}_3 = (0, 0, \sqrt{a^2 + b^2})$	Tetragonal body-centred (if $a \neq b$) Cubic primitive (if $a = b$)
Orthorhombic body-centred	$\boldsymbol{g}_1 = (1, 0, 1)$ $\boldsymbol{g}_2 = (0, -1, 1)$ $\boldsymbol{g}_3 = (1, -1, 0)$	Cubic body-centred
Orthorhombic face-centred	$\boldsymbol{g}_1 = (1/a, 1/b, 1/c)$ $\boldsymbol{g}_2 = (-1/a, -1/b, 1/c)$ $\boldsymbol{g}_3 = (1/a, -1/b, -1/c)$	
Tetragonal primitive	$\boldsymbol{g}_1 = (1, 0, 0)$ $\boldsymbol{g}_2 = (0, 1, 0)$ $\boldsymbol{g}_3 = (0, 0, 1)$	Cubic primitive
Tetragonal body-centred	$\boldsymbol{g}_1 = (0, 1, 1)$ $\boldsymbol{g}_2 = (1, 0, 1)$ $\boldsymbol{g}_3 = (1, 1, 0)$	Cubic body-centred
Trigonal primitive	$\boldsymbol{g}_1 = (0, -2/(3a), 1/(3c))$ $\boldsymbol{g}_2 = (1/(\sqrt{3}a), 1/(3a), 1/(3c))$ $\boldsymbol{g}_3 = (-1/(\sqrt{3}a), 1/(3a), 1/(3c))$	
Hexagonal primitive	$\boldsymbol{g}_1 = (1/(\sqrt{3}), -1, 0)$ $\boldsymbol{g}_2 = (2/(\sqrt{3}), 0, 0)$ $\boldsymbol{g}_3 = (0, 0, 2/(\sqrt{3}))$	Tetragonal body-centred
Cubic primitive	$\boldsymbol{g}_1 = (1, 0, 0)$ $\boldsymbol{g}_2 = (0, 1, 0)$ $\boldsymbol{g}_3 = (0, 0, 1)$	
Cubic face-centred	$\boldsymbol{g}_1 = (-1, 1, 1)$ $\boldsymbol{g}_2 = (1, -1, 1)$ $\boldsymbol{g}_3 = (1, 1, -1)$	
Cubic body-centred	$\boldsymbol{g}_1 = (0, 1, 1)$ $\boldsymbol{g}_2 = (1, 0, 1)$ $\boldsymbol{g}_3 = (1, 1, 0)$	

Table 2. Three dimensional Bravais lattice classes that are achievable using standing acoustic waves. The parameters a, b, and c are the lengths of the sides of the conventional unit cell for the Bravais lattice when they can be adjusted. The reciprocal lattice vectors we give satisfy $|\boldsymbol{g}_1| = |\boldsymbol{g}_2| = |\boldsymbol{g}_3|$ and need to be rescaled so that they have length k in order for them to be the wavevectors needed to realize a particular Bravais lattice. The angle γ is the angle between two of the sides of the conventional unit cell.

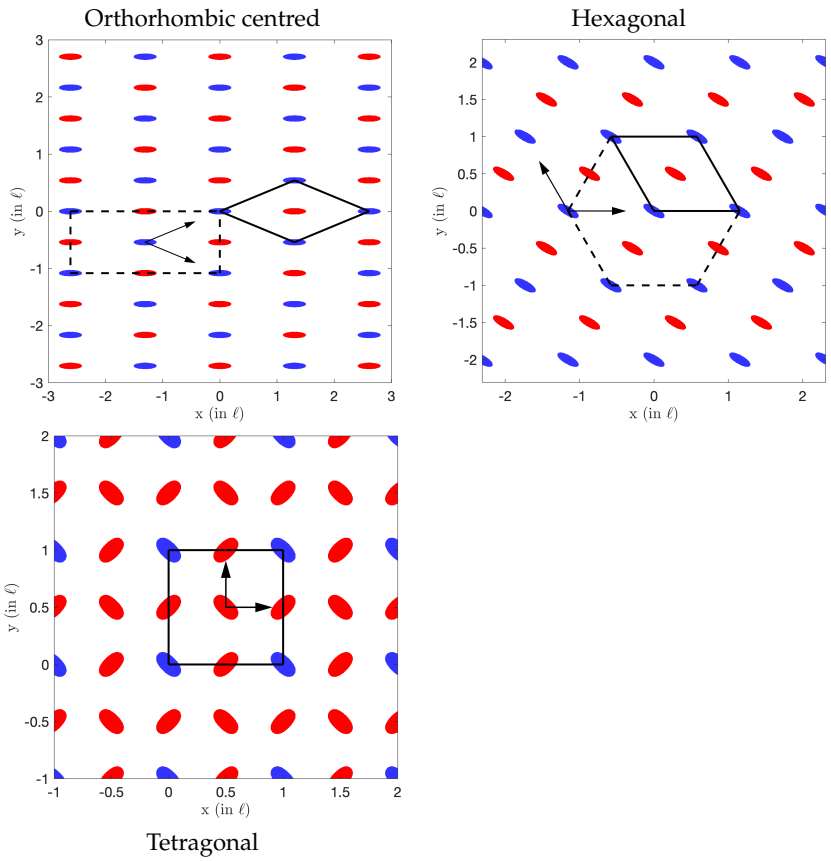

Figure 7. Representatives of the three Bravais lattice classes that are achievable in two dimensions. The classes are: orthorhombic centred ($\gamma = \pi/4$), hexagonal, and tetragonal. A primitive cell and unit cell are shown in black (note the primitive cell and the unit cell are identical for the tetragonal case). The coloured regions represent areas where the acoustic radiation potential is less than $\lambda_{\min} + 0.1(\lambda_{\max} - \lambda_{\min})$ and $\lambda_{\min}$ (resp. $\lambda_{\max}$) are the minimum (resp. maximum) eigenvalues of $\mathsf{Q}(\mathbf{0})$. The blue regions are the expected locations of minima due to the prescribed minimum location (the origin). The red regions are other minima that appear in the process. In all figures, the acoustic radiation potential parameters are $\mathfrak{a} = \mathfrak{b} = 1$. The black arrows indicate the directions normal to the transducer surfaces.

9. Collins DJ, Morahan B, Garcia-Bustos J, Doerig C, Plebanski M, Neild A. 2015 Two-dimensional single-cell patterning with one cell per well driven by surface acoustic waves. *Nature Communications* **6**, 8686 EP –.
10. Armstrong JPK, Puetzer JL, Serio A, Guex AG, Kapnisi M, Breant A, Zong Y, Assal V, Skaalure SC, King O, Murty T, Meinert C, Franklin AC, Bassindale PG, Nichols MK, Terracciano CM, Hutmacher DW, Drinkwater BW, Klein TJ, Perriman AW, Stevens MM. 2018 Engineering Anisotropic Muscle Tissue using Acoustic Cell Patterning. *Advanced Materials* **30**, 1802649.
11. Greenhall J, Raeymaekers B. 2017 3D Printing Macroscale Engineered Materials Using Ultrasound Directed Self-Assembly and Stereolithography. *Advanced Materials Technologies* **2**, 1700122–n/a. 1700122.
12. Caleap M, Drinkwater BW. 2014 Acoustically trapped colloidal crystals that are reconfigurable in real time. *Proceedings of the National Academy of Sciences* **111**, 6226–6230.
13. Silva GT, Lopes JH, Leão Neto JP, Nichols MK, Drinkwater BW. 2019 Particle Patterning by Ultrasonic Standing Waves in a Rectangular Cavity. *Phys. Rev. Applied* **11**, 054044.
14. Colton D, Kress R. 1998 *Inverse acoustic and electromagnetic scattering theory* vol. 93*Applied Mathematical Sciences*. Springer-Verlag, Berlin second edition.
15. Gor'kov LP. 1962 On the Forces Acting on a Small Particle in an Acoustical Field in an Ideal

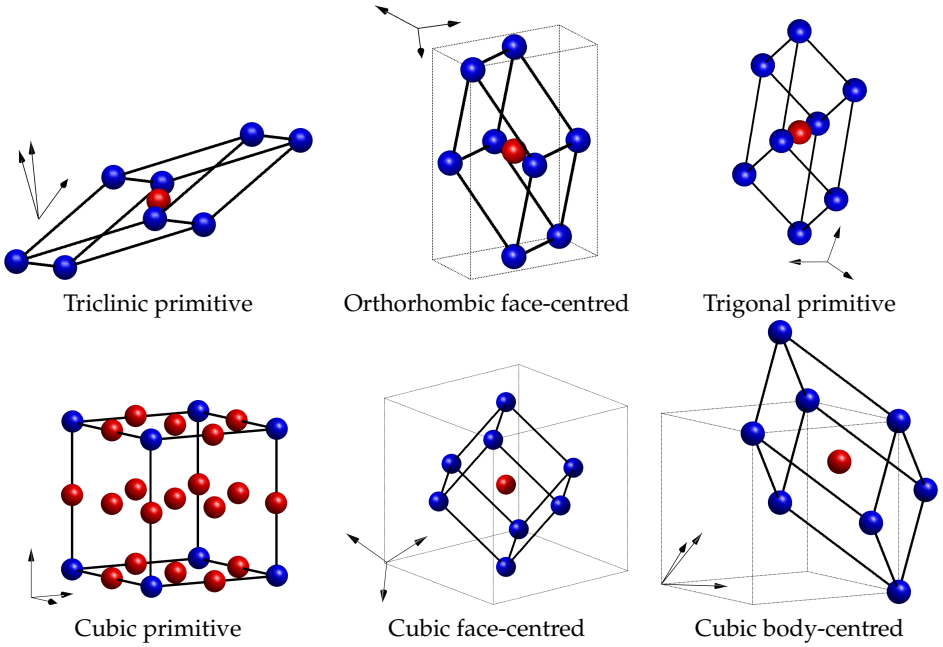

Figure 8. Representatives of the six achievable 3D Bravais lattice classes. The classes are: triclinic primitive ($\boldsymbol{g}_1 = (1, 2, 7), \boldsymbol{g}_2 = (8, 3, 5), \boldsymbol{g}_3 = (1, 3, 5)$), orthorhombic face-centred ($a = 1, b = 2, c = 3$), trigonal primitive ($a = 1, c = 2$), cubic primitive, cubic face-centred, and cubic body-centred. The primitive cell is shown in black. The blue regions are the expected locations of minima due to the prescribed minimum location (the origin). The red regions are other minima that appear in the process. In all figures, the acoustic radiation potential parameters are $\mathfrak{a} = \mathfrak{b} = 1$. The black arrows indicate the directions normal to the transducer surfaces.

Fluid. *Soviet Physics Doklady* **6**, 773.
16. King LV. 1934 On the Acoustic Radiation Pressure on Spheres. *Proceedings of the Royal Society of London A: Mathematical, Physical and Engineering Sciences* **147**, 212–240.
17. Bruus H. 2012 Acoustofluidics 7: The acoustic radiation force on small particles. *Lab Chip* **12**, 1014–1021.
18. Settnes M, Bruus H. 2012 Forces acting on a small particle in an acoustical field in a viscous fluid. *Phys. Rev. E* **85**, 016327.
19. Neuman KC, Block SM. 2004 Optical trapping. *Review of Scientific Instruments* **75**, 2787–2809.
20. Nieminen TA, Knöner G, Heckenberg NR, Rubinsztein-Dunlop H. 2007 Physics of optical tweezers. *Methods in cell biology* **82**, 207–236.
21. Thomas JL, Marchiano R, Baresch D. 2017 Acoustical and optical radiation pressure and the development of single beam acoustical tweezers. *Journal of Quantitative Spectroscopy and Radiative Transfer* **195**, 55 – 65. Laser-light and Interactions with Particles 2016.
22. Burns MM, Fournier JM, Golovchenko JA. 1990 Optical Matter: Crystallization and Binding in Intense Optical Fields. *Science* **249**, 749–754.
23. Hemmerich A, Zimmermann C, Hänsch TW. 1993 Sub-kHz Rayleigh Resonance in a Cubic Atomic Crystal. *Europhysics Letters (EPL)* **22**, 89–94.
24. Grynberg G, Lounis B, Verkerk P, Courtois JY, Salomon C. 1993 Quantized motion of cold cesium atoms in two- and three-dimensional optical potentials. *Phys. Rev. Lett.* **70**, 2249–2252.
25. Petsas KI, Coates AB, Grynberg G. 1994 Crystallography of optical lattices. *Phys. Rev. A* **50**, 5173–5189.
26. Cai LZ, Yang XL, Wang YR. 2002 All fourteen Bravais lattices can be formed by interference of four noncoplanar beams. *Opt. Lett.* **27**, 900–902.
27. Lee KL, Grémaud B, Han R, Englert BG, Miniatura C. 2009 Ultracold fermions in a graphene-type optical lattice. *Phys. Rev. A* **80**, 043411.
28. Kittel C. 2005 *Introduction to Solid State Physics*. John Wiley & Sons, Inc. 8th edition.

29. Besicovitch AS. 1940 On the linear independence of fractional powers of integers. *J. London Math. Soc.* **15**, 3–6.
30. Bohr H. 1947 *Almost Periodic Functions*. Chelsea Publishing Company, New York, N.Y.
31. Bradley CJ, Cracknell AP. 2010 *The mathematical theory of symmetry in solids*. Oxford Classic Texts in the Physical Sciences. The Clarendon Press, Oxford University Press, New York. Representation theory for point groups and space groups, Corrected paperback edition of the 1972 original.